The Journal of Neuroscience, July 15, 1996, *16*(14):4468–4478

Localization of the Somatostatin Receptor SST_{2A} in Rat Brain Using a Specific Anti-Peptide Antibody

Pascal Dournaud,[1] Yi Z. Gu,[3] Agnes Schonbrunn,[3] Jean Mazella,[1] Gloria S. Tannenbaum,[1,2] and Alain Beaudet[1]

Departments of [1]Neurology and Neurosurgery and [2]Pediatrics, McGill University, Montréal, Québec, Canada H3A 2B4, and [3]Department of Pharmacology, University of Texas, Houston Medical School, Houston, Texas 77225

Biological actions of somatostatin are exerted via a family of receptors, for which five genes recently have been cloned. However, none of these receptor proteins has been visualized yet in the brain. In the present study, the regional and cellular distribution of the somatostatin sst_{2A} receptor was investigated via immunocytochemistry in the rat central nervous system by using an antibody generated against a unique sequence of the receptor protein. Specificity of the antiserum was demonstrated by immunoblot and immunocytochemistry on rat brain membranes and/or on cells transfected with cDNA encoding the different sst receptor subtypes. In rat brain sections, sst_{2A} receptor immunoreactivity was concentrated either in perikarya and dendrites or in axon terminals distributed throughout the neuropil. Somatodendritic labeling was most prominent in the olfactory tubercle, layers II–III of the cerebral cortex, nucleus accumbens, pyramidal cells of CA1–CA2 subfields of the hippocampus, central and cortical amygdaloid nuclei, and locus coeruleus. Labeled terminals were detected mainly in the endopiriform nucleus, deep layers of the cortex, claustrum, substantia innominata, subiculum, basolateral amygdala, medial habenula, and periaqueductal gray. Electron microscopy confirmed the association of sst_{2A} receptors with perikarya and dendrites in the former regions and with axon terminals in the latter. These results provide the first characterization of the cellular distribution of a somatostatin receptor in mammalian brain. The widespread distribution of the sst_{2A} receptor in cerebral cortex and limbic structures suggests that it is involved in the transduction of both pre- and postsynaptic effects of somatostatin on cognition, learning, and memory.

Key words: immunohistochemistry; somatostatin; receptor; transfected cells; electron microscopy; central nervous system

Somatostatin (SRIF) is a tetradecapeptide present throughout the neuroaxis in which it is known to play both a neuroendocrine and a neurotransmitter role with diverse physiological effects on hormone release and cognitive and behavioral functions (for review, see Epelbaum et al., 1994). SRIF also has been shown to have antiproliferative actions on tumoral cells (Lamberts et al., 1991) and to be perturbed in certain neurological disorders including epilepsy, depression, and Alzheimer's disease (Epelbaum et al., 1994). The numerous functional effects of SRIF are exerted via G-protein-coupled receptors (Koch and Schonbrunn, 1984; Koch et al., 1985) for which five different genes recently have been cloned (Bruno et al., 1992; O'Carroll et al., 1992; Yamada et al., 1992; Yasuda et al., 1992). These receptors, designated sst_1 through sst_5 (Hoyer et al., 1995), bind SRIF-14 and its N-terminal extended form SRIF-28 with comparable affinity. The sst_2 receptor exists in two variant forms, sst_{2A} and sst_{2B}, generated by alternative splicing of the sst_2 mRNA (Vanetti et al., 1992, 1994). The two sst_2 receptor variants exhibit indistinguishable binding properties but may differ in G-protein coupling and desensitization (Reisine et al., 1993; Vanetti et al., 1993). Experiments on transfected cells suggest that sst_2, sst_3, and sst_5 receptors are equivalent pharmacologically to the SRIF-1 class of receptors, previously defined on the basis of their high affinity for the synthetic SRIF agonists MK 678 and octreotide, whereas sst_1 and sst_4 are equivalent to the SRIF-2 class, which lacks affinity for these compounds (for review, see Hoyer et al., 1994; Reisine and Bell, 1995).

The mRNAs for all five SRIF receptors are expressed widely in the human and rodent central nervous system (Breder et al., 1992; Kluxen et al., 1992; Kong et al., 1994; Pérez et al., 1994; Senaris et al., 1994; Beaudet et al., 1995). Although earlier autoradiographic receptor binding studies have examined the overall distribution of SRIF binding sites in mammalian brain and have distinguished between SRIF-1 and SRIF-2 pharmacological subtypes (Krantic et al., 1992), the relative abundance and localization of the different SRIF receptor proteins is unknown still. Furthermore, nothing is known of their cellular distribution, which is critical for understanding the modes of action of SRIF in the brain. In the present study, we have developed an antiserum against the sst_{2A} receptor and used it to characterize the regional and cellular localization of the sst_{2A} receptor protein in the rat brain.

MATERIALS AND METHODS

Antibody preparation and immunoblot analysis. Polyclonal antibodies were generated in New Zealand white rabbits against the peptide CERSDSKQDKSRLNETTETQRT after conjugation to keyhole limpet hemocyanin via the NH_2-terminal cysteine using m-maleimidobenzoyl-*N*-hydroxysuccinimide (Lerner et al., 1981). This sequence is located in the C-terminal region of the rat sst_{2A} receptor (Kluxen et al., 1992) and is

Received Feb. 5, 1996; revised April 22, 1996; accepted April 24, 1996.

This work was supported by grants from the Fonds de la Recherche en Santé du Québec and the Medical Research Council of Canada to G.S.T. and A.B., and from National Institutes of Health to A.S. G.S.T. is the recipient of a "Chercheur de Carrière" award from the Fonds de la Recherche en Santé du Québec. We thank F. Jiang, A. Morin, L. Mulcahy, D. Nouel, Y. Wang, and E. Di Camillo for their excellent assistance.

Correspondence should be addressed to Alain Beaudet, Montreal Neurological Institute, McGill University, Montréal, Québec, Canada H3A 2B4.

Dr. Dournaud's present address: Institut National de la Santé et de la Recherche Médicale, U-159, 2 Rue D'Alesia, 75014 Paris, France.

conserved in the mouse and human forms. Antibody specificity was determined by using CHO-K1 cells stably transfected with receptor subtypes sst_1 and sst_{2A} (provided by Dr. P.J.S. Stork), sst_{2B} (provided by Dr. V. Hollt), sst_3 (provided by Dr. Y. Patel), sst_4 (provided by Dr. M. Berelowitz), and sst_5 (provided by Dr. S. Seino). Membranes from CHO cells were prepared as described previously (Brown et al., 1990) and confirmed to bind specifically [^{125}I-Tyr^{11}]$SRIF_{14}$.

Rat cortical and cerebellar membranes were prepared from female Harlan Sprague–Dawley rats according to the protocol of Sakamoto et al. (1988) with minor changes. In brief, brain tissue was suspended in 10 vol of Tris buffer (50 mM Tris-Cl, pH 7.5, 5 mM $MgCl_2$, 1 mM EGTA, 200 μg/ml bacitracin, 0.5 μg/ml aprotonin, 10 μg/ml trypsin inhibitor, and 4 μg/ml PMSF) and homogenized with a polytron homogenizer at 900 rpm for 20 strokes. The membrane pellet obtained by high-speed centrifugation was stored at −70°C.

For immunoblot analysis, thawed membranes were pelleted in a microcentrifuge, resuspended in sample buffer (62.5 mM Tris-Cl, pH 6.8, 2% SDS, 20% glycerol, and 50 mM dithiothreitol), and electrophoresed on 10% SDS-acrylamide gels according to the method of Laemmli (1970). Proteins were transferred electrophoretically to PVDF membranes (0.2 μm; Bio-Rad, Mississauga, Ontario, Canada) in transfer buffer (10 mM $NaHCO_3$, 3 mM Na_2CO_3, 0.1% SDS, and 20% methanol). The membranes were blocked with 5% nonfat dry milk in PBS (10 mM Na_2HPO_4, pH 7.5, and 150 mM NaCl) for 2 hr at room temperature (RT) and then incubated overnight at 4°C with the anti-peptide antiserum diluted to between 1:10,000 and 1:20,000 in 1% nonfat dry milk containing 0.05% NaN_3. Immunoreactive bands were detected by incubating washed membranes for 1 hr with goat anti-rabbit IgG conjugated with horseradish peroxidase (1:10,000) (Bio-Rad) and developing with the Amersham (Oakville, Ontario, Canada) ECL kit according to the manufacturer's directions.

Immunocytochemical characterization of the antiserum. COS-7 cells were grown in DMEM containing glutamine supplemented with 44 mM $NaHCO_3$ and 10% fetal calf serum in the presence of 50 mg/ml gentamicin. Transient transfections were performed with 1 μg of recombinant plasmids for mouse sst_1, sst_{2A}, and sst_{2B} receptors (provided by Dr. T. Reisine) by the DEAE-dextran precipitation procedure (Perlman et al., 1992) onto semiconfluent COS-7 cells grown in 100 mm cell culture dishes. Sixty hours after transfections, cells were treated or not for 24 hr with 50 ng/ml pertussis toxin (Sigma, St. Louis, MO; Koch et al., 1985), fixed with 4% paraformaldehyde in 0.1 M phosphate buffer, pH 7.4, and incubated for 16 hr at RT with the R2-88 antiserum diluted 1:4000 in 0.1 M TBS containing 1% normal goat serum (ngs) in the presence or absence of 0.1% Triton X-100. After rinsing, cells were incubated for 1 hr at RT with a 1:200 dilution of conjugated Texas Red-goat anti-rabbit IgG (Jackson ImmunoResearch, West Grove, PA), washed several times in 0.1 M TBS, and examined by confocal microscopy using a Leica inverted microscope equipped with a krypton laser. Fluorescence intensity measurements were performed on 12 pertussis toxin-treated and untreated cells using the Leica software package. Results are expressed as gray level units on a 0–255 gray scale.

Immunocytochemistry. Adult male Sprague–Dawley rats (150–200 gm body weight) were anesthetized with Somnotol (MTC Pharmaceuticals; 80 mg/kg, i.p.) and perfused transaortically with 4% paraformaldehyde in 0.1 M TBS. Brains were post-fixed for 60 min in the same fixative, cryoprotected, and frozen in liquid isopentane at −45°C. Immunocytochemical experiments were performed by using the avidin-biotinylated-peroxidase complex (ABC) standard kit (Vector Laboratories, Burlingame, CA) and a biotinyl-tyramide amplification system (DuPont NEN, Wilmington, DE). Briefly, 30 μm sections were preincubated for 30 min in TBS containing 3% ngs and incubated for 16 hr at RT in a 1:1000 dilution of the R2-88 antiserum containing 0.2% Triton X-100. Then sections were rinsed in 0.1 M TBS and incubated sequentially for 45 min in biotinylated goat anti-rabbit IgG (Jackson ImmunoResearch) diluted 1:100 in 0.1 M TBS and in ABC solution. Then they were incubated for 10 min in a 0.01% biotinyl-tyramide solution (Adams, 1992), activated with 0.01% H_2O_2, and then reincubated in ABC solution. Visualization of the bound peroxidase was achieved by reaction in a solution of 0.1 M Tris buffer containing 0.05% 3,3′ diaminobenzidine (DAB), 0.04% nickel chloride, and 0.01% H_2O_2. Immunolabeling for electron microscopy was performed as above, except that glutaraldehyde (0.2%) was added to the fixative, and the tissue was sectioned on a Vibratome. Immunoreacted sections taken at the level of the hippocampal formation, amygdaloid complex, and medial habenula were post-fixed for 1 hr in 2% osmium tetroxide, dehydrated in graded ethanols, embedded in Epon, sectioned with an ultramicrotome, counterstained with lead citrate, and examined with a Jeol 100CX electron microscope.

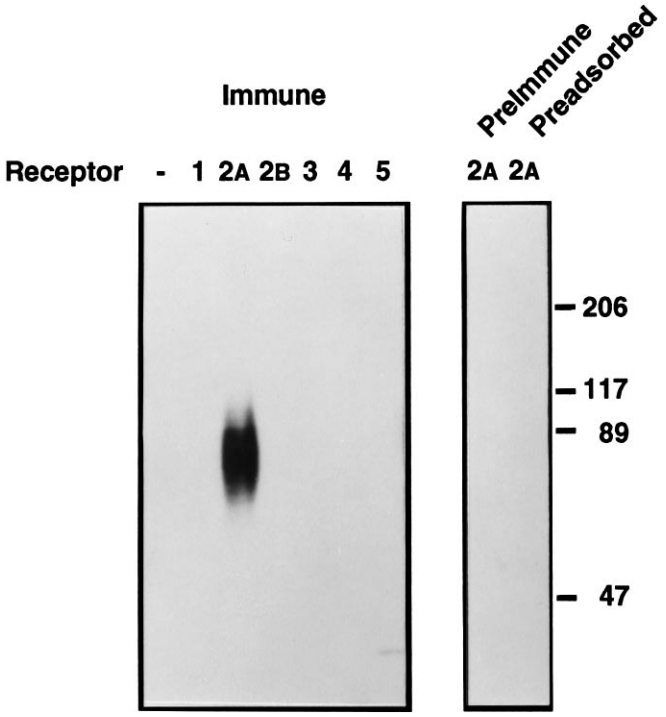

Figure 1. Western blot analysis of R2-88 immunoreactivity in CHO-K1 cells. Membranes (40 μg) from either parental CHO-K1 cells or from CHO-K1 cells transfected with cDNA encoding individual sst receptor subtypes were separated on SDS-PAGE. After transfer to PVDF membranes, the proteins were immunoblotted with a 1:10,000 dilution of R2-88 immune serum (*Immune*), R2-88 preimmune serum (*PreImmune*), or R2-88 immune serum in the presence of 1 μM peptide antigen (*Preadsorbed*). Molecular size markers (in kDa) are shown on the *right*.

Controls. For controls, the R2-88 antiserum was adsorbed with an excess of sst_{2A} carboxyl-terminal peptide, or the immune serum was replaced by R2-88 preimmune serum. In addition, a method specificity control was performed by omitting the antiserum from the immunohistochemical staining protocol.

RESULTS

Immunoblot analysis

The anti-peptide antiserum R2-88 reacted strongly with a broad band of ~85 kDa in CHO-K1 cells stably transfected with a rat sst_{2A}-receptor expression plasmid (Fig. 1). The immunoreactivity was abolished completely when the staining was performed in the presence of 1 μM peptide antigen or with preimmune in lieu of immune serum, demonstrating that it was produced by the anti-peptide antibodies (Fig. 1). The antiserum did not react with the parental cells, which do not express sst receptors, nor with sst receptors from cells transfected with any of the other receptor subtypes, demonstrating that it was specific for the sst_{2A} receptor (Fig. 1). In separate experiments, R2-88 antiserum was found to immunoprecipitate the sst_{2A} receptor with 60–80% efficiency and to precipitate <1% of any of the other receptor subtypes (Schonbrunn et al., 1995).

To determine whether the antiserum specifically recognized the sst_{2A} receptor protein in brain tissue, we compared the immunoreactivity present in membranes from rat cerebral cortex, which contains high levels of sst_2 receptor mRNA, with that from rat cerebellum, which contains no or only low levels of sst_2 receptor mRNA (Breder et al., 1992; Kong et al., 1994; Perez et al., 1994;

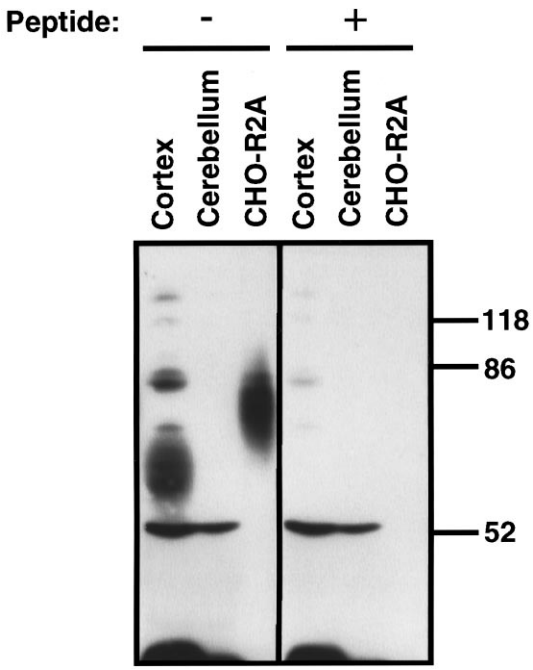

Figure 2. Western blot analysis of R2-88 immunoreactivity in rat brain. Membranes from rat cerebral cortex (50 μg), rat cerebellum (50 μg), or CHO-R2A cells (25 μg) were separated on a 10% SDS-acrylamide gel. After transfer to PVDF membranes, the proteins were immunoblotted with a 1:20,000 dilution of R2-88 immune serum in the absence or presence of 1 nM peptide antigen, as indicated. Molecular size markers (in kDa) are shown on the *right*.

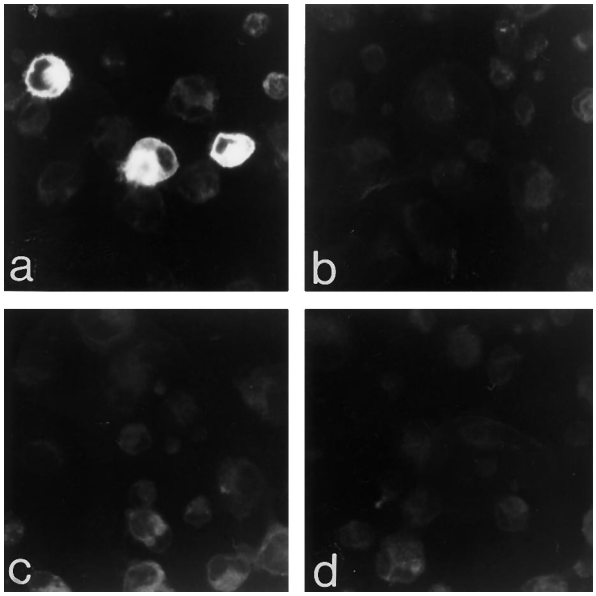

Figure 3. Confocal imaging of COS-7 cells immunocytochemically stained for the sst_{2A} receptor. COS-7 cells transiently transfected with cDNA encoding the sst_{2A} receptor exhibit intense cytoplasmic immunoreactivity (*a*). The yield of the transfection is ~20%, which explains the presence of nonlabeled cells in the same field. No labeled cells are apparent in preparations incubated with preimmune serum (*b*) or with the R2-88 immune serum preadsorbed with an excess of peptide antigen (*c*). COS-7 cells transfected with cDNA encoding the sst_{2B} receptor are immunonegative, also (*d*). Magnification, 300×.

Senaris et al., 1994). The antiserum reacted strongly with a broad 72 kDa band in cortical membranes (Fig. 2), consistent with the results from affinity cross-linking of rat cerebrocortical sst receptors (Sakamoto et al., 1988; Kimura, 1989). This staining was prevented by 1 nM peptide antigen and was not detected in cerebellar membranes (Fig. 2). Although several other bands were stained weakly by the antiserum, the lack of competition by peptide antigen indicated that their staining was caused by unrelated antibodies in the serum.

Visualization of sst_{2A} receptor in transfected cells

Approximately 20% of COS-7 cells transiently transfected with cDNA encoding the sst_{2A} receptor were immunolabeled intensely with the R2-88 antiserum (dilution, 1:4000; Fig. 3*a*), congruent with the reported transfection yield in this cell line (Pollard et al., 1984). By contrast, no immunoreaction product was detected in cells transfected with cDNA encoding the sst_1 (not shown), the sst_{2B} receptor (Fig. 3*d*), or in nontransfected cells. Immunolabeling was decreased greatly in the absence of detergent and abolished when the incubation was performed with either preimmune serum or with immune serum preadsorbed with 1 μM sst_{2A} antigenic peptide (Fig. 3*b,c*). Neither the number nor the labeling density of sst_{2A}-immunoreactive cells was modified by pretreatment of the cells with pertussis toxin (mean fluorescence intensity, 94.5 ± 5.8 vs 92 ± 7.3 gray level units for treated vs untreated cells, respectively).

Light microscopic localization of sst_{2A} receptor in rat brain

Rat brain sections immunoreacted with R2-88 antiserum exhibited selective patterns of immunostaining, the distribution of which closely resembled that of SRIF binding sites previously documented by using receptor autoradiography (Fig. 4*a,b*). This staining was absent in sections incubated either with preimmune serum, immune serum preadsorbed with sst_{2A} antigenic peptide (Fig. 4*c*), or in the absence of primary antibody. At high magnification, the immunostaining was seen to be associated either with neuronal perikarya and dendrites or with axon terminals, depending on the region examined (Table 1; Figs. 5–7). Perikaryal labeling pervaded the cytoplasm of the cells, sparing the nucleus; dendritic labeling was usually confined to primary or, more rarely, secondary branches (Figs. 6*D*, 7*C*). Axonal labeling took the form of a fine dusting of the neuropil (Figs. 5*D*, 7*B*), within which individually labeled punctae could be distinguished at high magnification (Fig. 6*B*). No sst_{2A} receptor immunolabeling was observed over glial cells.

Rostrally, numerous strongly immunoreactive nerve cell bodies and proximal dendrites were observed throughout the pyramidal layer of the olfactory tubercle, extending into the polymorph layer (Fig. 5*A*; Table 1). More sparse and less intensely reactive nerve cell bodies also were visible in layer II of the piriform cortex. Dense terminal labeling, but no labeled perikarya, was apparent in the endopiriform and anterior olfactory nuclei as well as in the lateral olfactory tract nucleus.

Both immunoreactive perikarya and immunoreactive terminal fields were detected throughout the neocortex, in which they assumed specific laminar distributions (Table 1). In the anterior cingulate and retrosplenial cortices, sst_{2A} immunoreactivity was concentrated mainly within nerve cell bodies in layer II (Fig. 5*B*). In the frontal, parietal, temporal, and occipital cortices, prominent perikaryal staining was observed in layers II–III (Fig. 5*C*). Most of these neurons extended labeled apical dendrites up to layer I. A few less intensely immunoreactive perikarya also were evident in layers V–VI (Fig. 5*C*). Most conspicuous in the latter

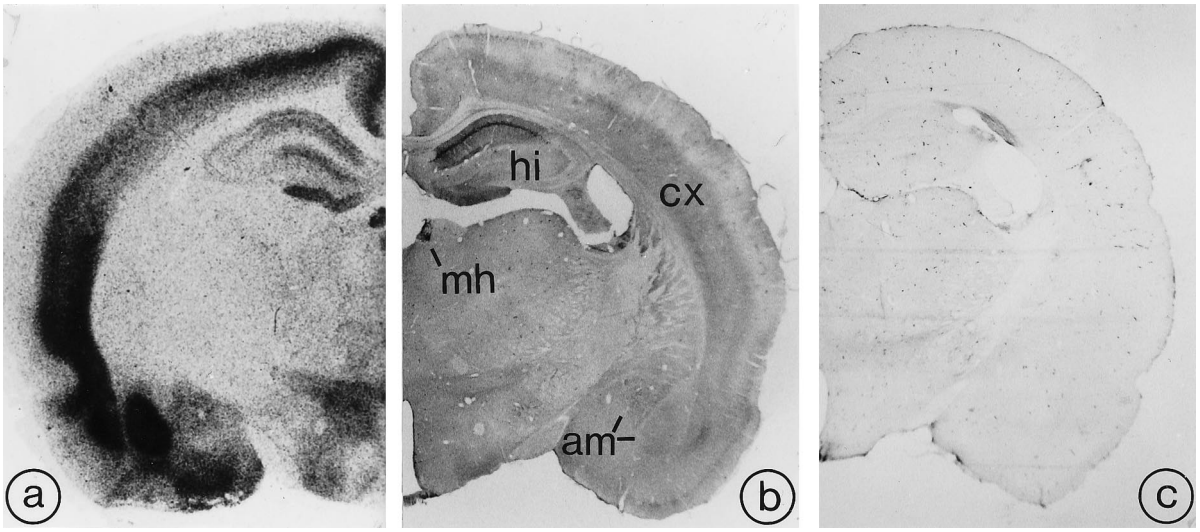

Figure 4. Comparative distribution of [^{125}I]SRIF binding sites (*a*) and sst_{2A} receptor immunoreactivity (*b*) in rat brain. Section in *c* was immunoreacted with R2-88 antiserum preadsorbed with an excess of the peptide antigen. *a*, Autoradiogram of a 20 μm rat midbrain section incubated with [^{125}I]-Tyr_0-$DTrp_8$-SRIF-14 for 45 min. Reproduced from Moyse et al. (1992), with permission. *b*, As for [^{125}I]SRIF binding, sst_{2A} receptor immunoreactivity predominates in the deep layers of the cortex (*cx*), the medial habenula (*mh*), the hippocampal formation (*hi*), and the amygdaloid complex (*am*). *c*, By comparison, the preadsorbed control is virtually devoid of immunoreactivity. Magnification, 7×.

layers, however, were immunoreactive terminal fields (Fig. 5*C*). Perirhinal and enthorinal cortices exhibited numerous labeled perikarya in layers II–III and dense terminal labeling in the outer portion of layer V and throughout layer VI (Fig. 5*D*).

High densities of immunoreactive perikarya and dendrites were detected in the lateral division of the bed nucleus of the stria terminalis (Fig. 6*A*; Table 1). Smaller and more sparsely distributed cells also were evident in the intermediate and ventral divisions of the nucleus, dorsal and ventral to the anterior commissure, respectively (Fig. 6*A*). In the medial habenular nucleus, immunoreactive cell bodies were distributed among a dense network of strongly immunoreactive processes (Fig. 6*B*). The lateral part of the nucleus was devoid of immunoreactivity.

Several small or medium-sized immunoreactive nerve cell bodies were evident throughout the ventrolateral and caudal segments of the neostriatum (Fig. 6*C*) as well as within the core and shell divisions of the nucleus accumbens (Table 1). Dense terminal labeling, but no immunoreactive perikarya, were visible in the claustrum. Highly arborized, densely immunoreactive cell bodies and dendrites were observed in the dorsolateral septum along the upper part of the third ventricle immediately beneath the corpus callosum (Fig. 6*D*).

Pyramidal cells in the CA1–CA2 fields of the hippocampus were labeled the most intensely and conspicuously in the brain (Fig. 7*A*; Table 1). Prominent labeling of their basal and apical dendrites was also evident in strata oriens and radiatum, respectively, superimposed over moderate terminal labeling (Fig. 7*C*). A few labeled perikarya also were observed in the stratum radiatum. No immunoreactive cell bodies, but diffuse neuropil labeling, was apparent in the stratum lacunosum moleculare (Fig. 7*A*). In contrast, the CA3 subfield remained consistently immunonegative. Diffuse terminal labeling was apparent in the molecular layer of the dentate gyrus as well as, albeit less prominently, at the granule cell–hilar border. Dense terminal labeling also was evident in the subiculum.

Both perikaryal and terminal labeling were detected in the amygdaloid complex, the former in the central and the latter in the basolateral nucleus (Fig. 7*B*). The medial and cortical amygdaloid nuclei exhibited weak-to-intense perikaryal immunostaining, whereas the lateral amygdaloid nucleus was immunonegative.

Only sparse sst_{2A} receptor-immunoreactive nerve cell bodies were detected within the hypothalamus, and these usually were stained lightly except in the tuberomammillary nucleus in which they formed a tight cluster of moderately immunoreactive cells. Diffuse terminal labeling was apparent in a few hypothalamic nuclei, including the paraventricular and the arcuate nuclei (Table 1).

In the midbrain, selectively labeled nerve cell bodies were apparent in the deep layers of the superior colliculi and in the periaqueductal gray matter (Table 1). Many of these neurons were observed to extend long and fine processes. Additionally, moderately dense terminal labeling was evident in the dorsal and lateral segment of the periaqueductal gray, gray layers of the superior colliculus, pars compacta of the substantia nigra, and ventral tegmental area.

In the pons, intensely labeled perikarya and processes were detected throughout the locus coeruleus (Fig. 7*D*). Less intensely labeled neurons also were visible in the lateral dorsal tegmental and parabrachial nuclei. In the medulla, immunoreactive nerve cell bodies were most evident in the dorsal motor nucleus of the vagus and lateral reticular nucleus, and immunoreactive axons were observed in the nucleus tractus solitarius and medial vestibular nucleus. Both the cerebellar cortex and deep cerebellar nuclei were devoid of immunostaining (Table 1).

Electron microscopic localization of sst_{2A} receptor in selected limbic structures

Electron microscopy confirmed the association of immunoreactivity with neuronal perikarya and dendrites in the hippocampus, medial habenula, and central amygdaloid nucleus (Fig. 8*A,B*) and with axon terminals in the medial habenula and basolateral amygdala (Fig. 8*C*). In perikarya and processes alike, the reaction product pervaded the cytoplasm as opposed to being confined to the plasma membrane. Labeled dendrites often were varicose and

Table 1. Distribution of sst_{2A}-like immunoreactivity in rat brain*

Region	Perikarya and dendrites	Axon terminals
Telencephalon		
Olfactory system		
Olfactory tubercle	+++	−
Piriform cortex	++	+
Endopiriform nucleus	−	+++
Anterior olfactory nucleus	−	++
Lateral olfactory tract nucleus	−	++
Cerebral cortex		
Layer I	−	−/+
Layers II–III	++	−
Layers V–VI	+	+++
Basal forebrain		
Bed nucleus stria terminalis	+++	−
Diagonal band of Broca (vertical limb)	+	−
Substantia innominata	−	+++
Basal ganglia		
Medial caudoputamen	+	−
Caudal caudoputamen	++	−
Fundus striati	++	−
Core accumbens	++	−
Shell accumbens	++	−
Claustrum	−	+++
Dorsolateral septum	++	+/++
Hippocampal formation		
CA1–2 area		
Stratum oriens	−/+	++
Stratum pyramidale	+++	−
Stratum radiatum	+	++
Stratum lacunosum moleculare	−	+++
Dentate gyrus		
Molecular layer (ventral part)	−	++
Hilus	−	−/+
Subiculum	−	+++
Amygdala		
Central amygdaloid nucleus	+++	−
Basolateral amygdaloid nucleus	−/+	+++
Medial amygdaloid nucleus	++	−
Cortical amygdaloid nucleus	+++	−
Diencephalon		
Medial habenula	++	+++
Paraventricular thalamus	−	+
Zona incerta	−	+
Hypothalamus		
Medial preoptic area	−/+	+
Periventricular nucleus	−/+	+
Paraventricular nucleus	−	+/++
Ventromedial nucleus	+	−
Arcuate nucleus	−/+	+/++
Median eminence	−	+
Tuberomammillary nucleus	++	−/+
Mesencephalon		
Superior colliculus		
Superficial gray	+	+++
Intermediate gray	+	++
Central gray	++	++/+++
Dorsal raphe nucleus	−	+
Substantia nigra (pars compacta)	−	+
Ventral tegmental area	−	+
Raphe linearis caudalis	−	+
Midbrain reticular formation	+	+
Pons		
Parabrachial nucleus	+	+
Lateral dorsal tegmental nucleus	++	−
Locus coeruleus	+++	++/+++
Medulla		
Nucleus tractus solitarius	+	++
Medial vestibular nucleus	−/+	++
Lateral reticular nucleus	+	−
Dorsal motor nucleus of the vagus	++	+
Cerebellum		
Cerebellar cortex	−	−
Deep cerebellar nuclei	−	−

*Relative values. Data based on light microscopic observations.

received both symmetric and asymmetric synaptic contacts from unlabeled axon terminals (Fig. 8*B*). Immunoreactive axon terminals were seen in synaptic contact with unlabeled dendrites (Fig. 8*C*) but not with other unlabeled terminals.

DISCUSSION

The present study provides the first description of the cellular distribution of an SRIF receptor protein in mammalian brain. The specificity of the antiserum was established initially by Western blot in membranes of CHO-K1 cells transfected with the cDNA encoding each of the different sst receptor subtypes. The antiserum recognized a broad protein band centered near 85 kDa in membranes from sst_{2A}-transfected CHO-K1 cells but did not react with CHO membranes containing any of the other receptor subtypes. This band had the same molecular weight and migration pattern as the photoaffinity-labeled receptor in the CHO-R2A cells, confirming that the detected protein represents the sst_{2A} receptor (Gu et al., 1995). The apparent molecular weight of this receptor protein is markedly higher than the 41.2 kDa predicted from the amino acid sequence (Kluxen et al., 1992), which is consistent with the hypothesis that the sst_{2A} receptor undergoes extensive post-translational modifications (Patel et al., 1994; Reisine and Bell, 1995). Further, the broad migration pattern is characteristic of heavily glycosylated proteins and has been observed with numerous other seven transmembrane domain receptors.

The specificity of the antibody for the sst_{2A} receptor in rat brain was characterized further by immunoblot in rat brain membranes. In agreement with previous cross-linking studies showing that affinity-labeled rat cerebrocortical SRIF receptors migrate as a broad band with an apparent molecular weight of ~72 kDa (Sakamoto et al., 1988; Kimura, 1989), our antibody specifically recognized a broad protein band centered near 72 kDa. For reasons not entirely clear, this molecular weight is considerably lower than that of 148 kDa previously reported for the sst_2 receptor detected in rat brain using an antibody directed against the third extracellular domain of the receptor (Theveniau et al., 1994). Our conclusion that the 72 kDa band represents the sst_{2A} receptor is supported by the fact that (1) antibody binding to this band was abolished by a concentration of peptide antigen as low as 1 nM, and (2) this band was not visible in rat cerebellar membranes that express low or undetectable levels of sst_{2A} mRNA (Kong et al., 1994; Perez et al., 1994; Senaris et al., 1994). The slightly lower apparent molecular weight of the labeled sst_{2A} receptor in cortex as compared with its molecular weight in CHO-R2A cells suggests that the sst_{2A} receptor is glycosylated less heavily in neurons than in transfected CHO cells.

Experiments on transfected COS-7 cells further confirmed the specificity of the R2-88 antiserum and indicated that it provided for selective detection of the sst_{2A} antigen in paraformaldehyde-fixed tissue. The lack of staining of sst_1- and sst_{2B}-transfected cells indicated further that the antiserum recognized specifically the C-terminal sequence of the sst_{2A} receptor, as expected from the amino acid sequence of the immunogenic peptide. The marked decrease in staining observed in the absence of detergent confirmed that the C-terminal tail is intracellular, as predicted from structural homology of the receptor with rhodopsin (Kluxen et al., 1992). Finally, the similarity in the pattern and intensity of immunostaining between cells treated or not with pertussin toxin indicated that our antibody recognized G-protein-coupled (Tomura et al., 1994) and uncoupled forms of the receptor equally well.

The regional distribution of the sst_{2A} receptor immunoreactiv-

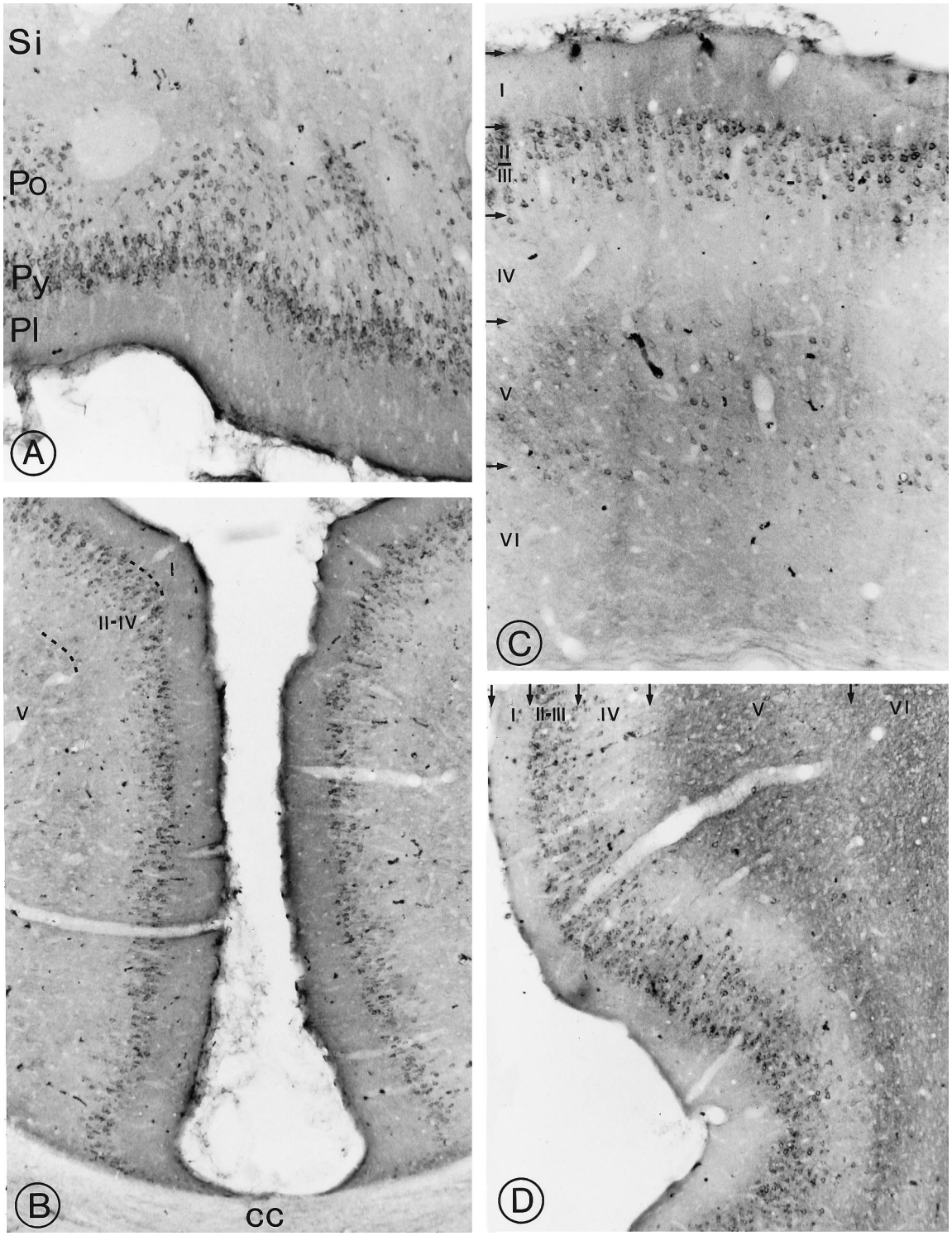

Figure 5. Light microscopic distribution of sst_{2A} receptor immunoreactivity in cerebral cortex. *A*, Olfactory tubercle. Perikaryal immunostaining is prominent in cell bodies in the pyramidal (*Py*) and polymorph (*Po*) cell layers. *Pl*, Plexiform layer; *Si*, substantia innominata. Magnification, 250×. *B*, Anterior cingulate cortex. Numerous sst_{2A}-immunoreactive perikarya are apparent throughout layer II. *cc*, Corpus callosum. Magnification, 170×. *C*, Parietal cortex. Immunoreactive nerve cell bodies are numerous in layers II–III and more sparsely distributed in layer V. Fields of labeled axon terminals are evident in deep layers, most prominently in layer V. Magnification, 270×. *D*, Dense perikaryal labeling is evident throughout layers II–III. Labeled terminal fields pervade the outer segment of layer V as well as layer VI. Magnification, 220×.

ity in rat brain sections was strikingly similar to that of SRIF binding sites previously documented by using receptor autoradiography (Martin et al., 1991; Krantic et al., 1992; Moyse et al., 1992) (see also Fig. 3). As expected, this distribution most closely paralleled that of the binding of SRIF agonists SMS 201–995 and MK 678 (Martin et al., 1991; Krantic et al., 1992), which recognize with high affinity the sst_2, sst_3, and sst_5 receptors. More surprisingly, it also correlated remarkably well with the binding patterns

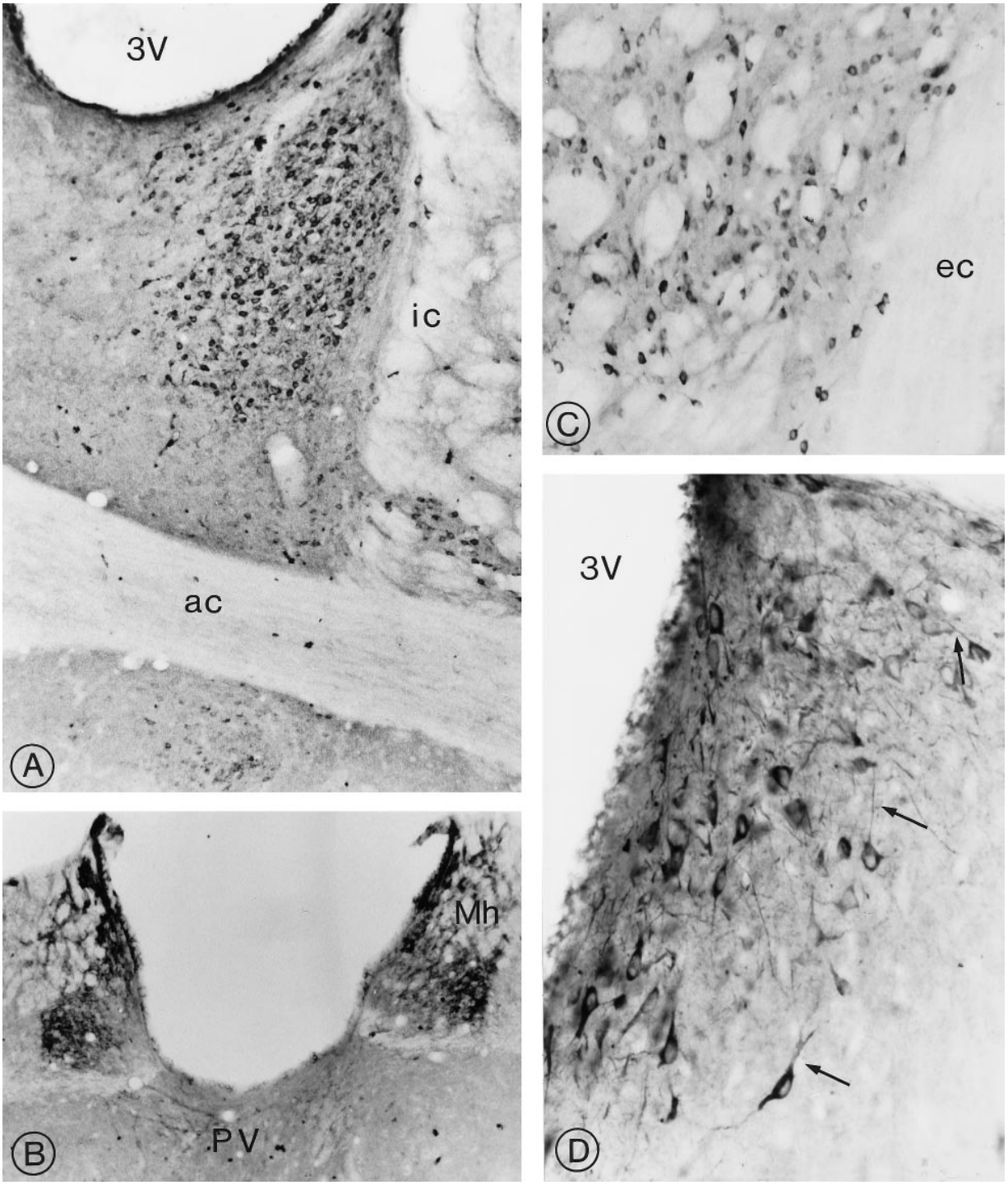

Figure 6. Distribution of sst_{2A} receptor immunoreactivity in the limbic system and neostriatum. *A*, Prominent perikaryal immunolabeling is detected throughout the lateral, intermediate, and ventral divisions of the bed nucleus of the stria terminalis. *ic*, Internal capsule; *ac*, anterior commissure; *3V*, third ventricle. Magnification, 220×. *B*, Intense immunolabeling of nerve cell bodies and intervening neuropil pervades the medial habenular nucleus (*Mh*). Note the absence of labeling in the lateral division of the nucleus and the presence of immunoreactive axon terminals in the paraventricular nucleus of the thalamus (*PV*). Magnification, 270×. *C*, Small, intensely immunoreactive spiny type I neurons are evident in between the myelinated fascicles of the internal capsule in the ventrolateral neostriatum. *ec*, External capsule. Magnification, 420×. *D*, Dorsolateral septum. The labeling clearly is seen to pervade the cytoplasm of neuronal perikarya and their proximal dendrites (*arrows*). *3V*, Third ventricle. Magnification, 850×.

of less selective ligands, such as iodinated SRIF-14, which have been shown to bind all sst subtypes (reviewed in Hoyer et al., 1994; Reisine and Bell, 1995). This correspondence suggests that SRIF receptors other than sst_{2A} are expressed either by subpopulations of the same cells or by subsets of neurons within the same regions.

At cellular and subcellular levels, sst_{2A} receptor immunoreactivity was concentrated in perikarya and dendrites as well as in

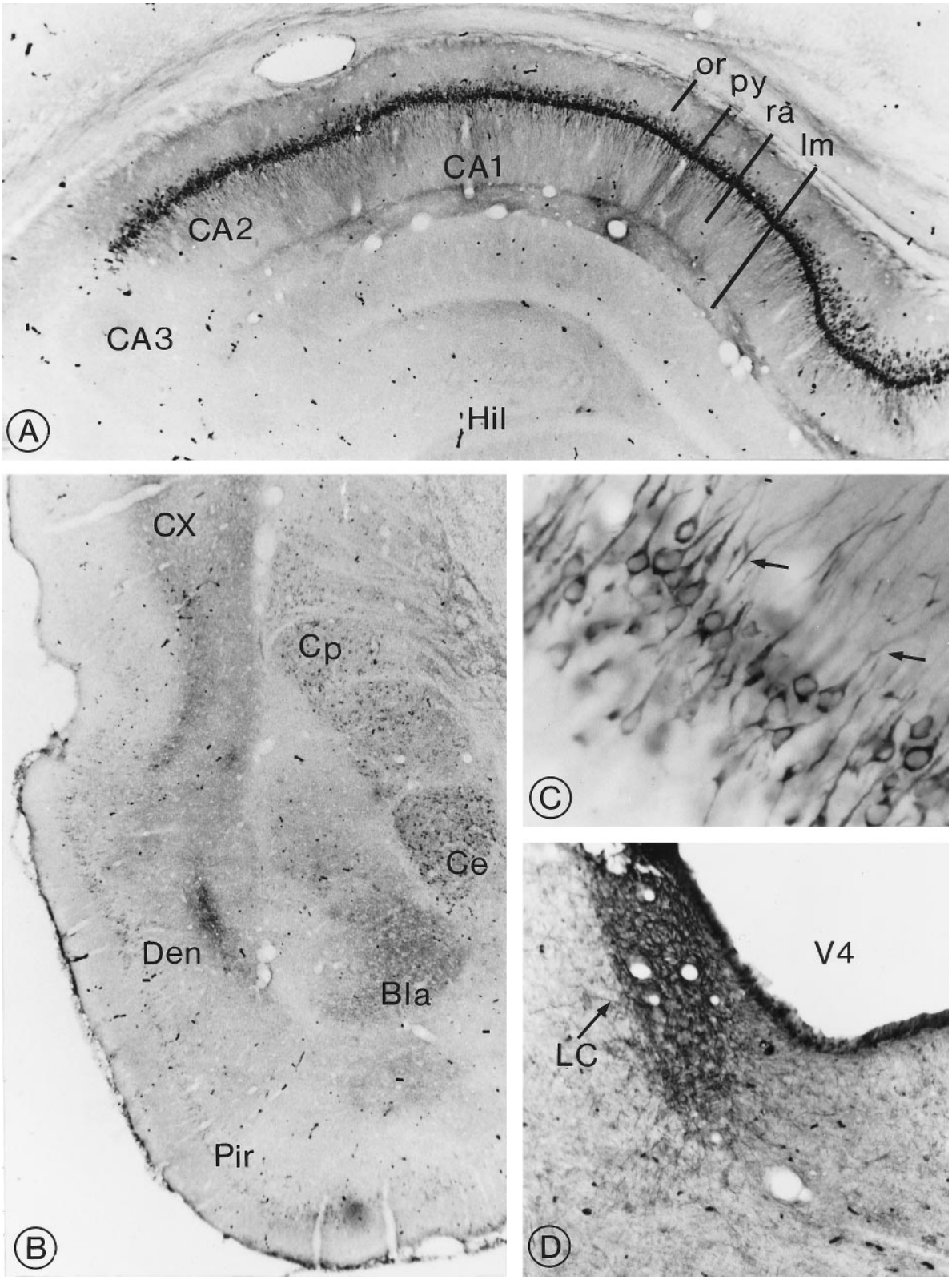

Figure 7. Distribution of sst_{2A} receptor immunoreactivity in the hippocampus, amygdala, and pons. *A*, Hippocampus. Intensely labeled pyramidal cells and proximal dendrites in subfields CA1–CA2 are superimposed over neuropil staining, stopping abruptly at CA3. *or*, Stratum oriens; *py*, stratum pyramidale; *ra*, stratum radiatum; *lm*, stratum lacunosum moleculare; *Hil*, hilus. Magnification, 140×. *B*, Temporal lobe. Intense immunoreactivity is evident in the central (*Ce*) and basolateral (*Bla*) amygdaloid nuclei. However, in the former, it is confined to nerve cell bodies and, in the latter, to axon terminals. Note the dense terminal labeling in the dorsal endopiriform nucleus (*Den*) and in the deep layers of the perirhinal cortex (*CX*). *Cp*, Caudate putamen; *Pir*, piriform cortex. Magnification, 100×. *E*, Labeled pyramidal cells in CA1. Apical dendrites are seen extending into the stratum radiatum (*arrows*). Note the sparing of the nucleus. Magnification, 1300×. *D*, Locus coeruleus (*LC*). Nerve cell bodies and surrounding neuropil are equally, densely immunoreactive. *V4*, 4th ventricle. Magnification, 100×.

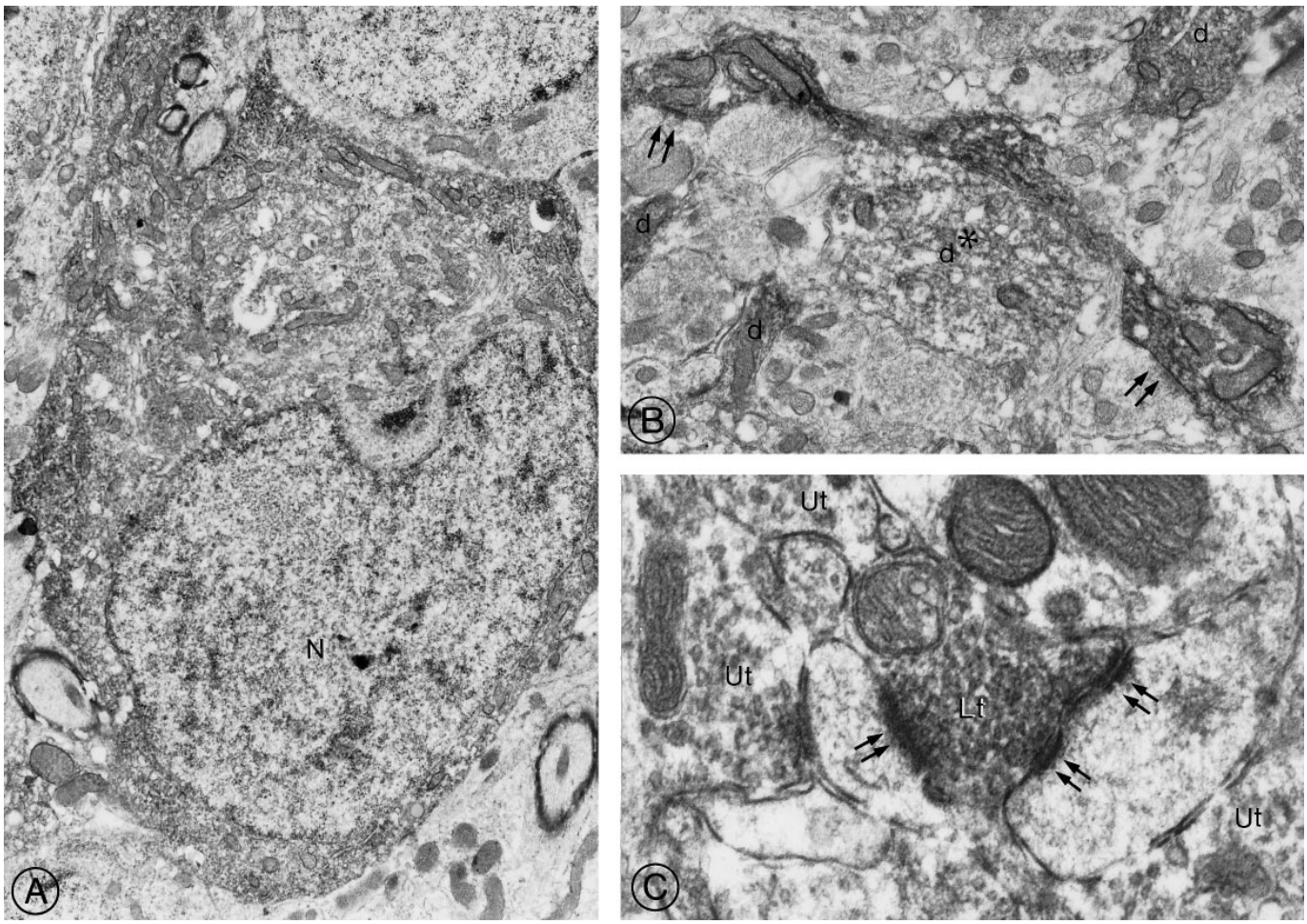

Figure 8. Electron microscopic detection of sst_{2A} receptor protein in rat brain. *A*, Neuronal perikaryon in the medial habenula. The reaction product pervades the entire cytoplasm but spares the nucleus. Magnification, 8000×. *B*, Large varicose dendrite in the medial habenula. Both the upper and the lower dilatations are in synaptic contact (*double arrows*) with unlabeled terminals. Note the four neighboring cross-sectioned immunoreactive dendrites (*d*). One of these dendrites (*) is labeled less intensely than the others and is apposed directly to the large varicose one. Magnification, 11,500×. *C*, Labeled axon terminal (*Lt*) detected among unlabeled ones (*Ut*) in the basolateral amygdala. The labeled terminal forms asymmetric synaptic contacts (*double arrows*) with two immunonegative dendrites. Magnification, 32,000×.

axon terminals profusely distributed in the neuropil. These findings demonstrate that the sst_{2A} receptor subtype is in a position to transduce both post- and presynaptic effects of SRIF in mammalian brain. The association of sst_{2A} receptor immunoreactivity with the somatodendritic arbor of neurons in the locus coeruleus, dorsolateral septum, CA1 subfield of the hippocampus, and the nucleus of the solitary tract observed in the present study is consistent with the postsynaptic electrophysiological effects of locally administrated SRIF documented within these areas (Olpe et al., 1987; Jacquin et al., 1988; Schweitzer et al., 1990, 1993; Twery et al., 1991; Xie and Sastry, 1992). By contrast, the extensive labeling of axonal fields suggests that presynaptic effects of SRIF in the rat brain may be more pervasive than earlier functional studies had led us to believe (Göthert, 1980; Tanaka and Tsujimoto, 1981). Interestingly, labeled terminals usually were distributed in nuclei distinct from those containing immunoreactive perikarya, suggesting that neurons harboring sst_{2A} receptors are mainly projection neurons.

In both COS-7 cells and rat brain sections, sst_{2A} receptor immunoreactivity was found by high resolution microscopy (confocal for the former and electron for the latter) to be associated not only with the inner plasma membrane but also with the cytoplasm of labeled cells. Similar intracytoplasmic localizations have been reported for other types of G-protein-coupled receptors (Levey et al., 1991, 1993; Sesack et al., 1994; Arvidsson et al., 1995) and may be attributed, in part, to artifactitious diffusion of the peroxidase complex from the membrane (Novikoff et al., 1972). This factor alone, however, would not explain the cytoplasmic labeling of COS-7 cells that were stained by immunofluorescence. It is therefore likely that part of the immunolabeling observed in the cytoplasm of both neurons and COS-7 cells represents neosynthesized, transported, and/or recycled receptors. These intracellular sites are likely to be in a different functional ligand-binding state than membrane-associated ones, because regions shown here to contain sst_{2A} receptor-immunoreactive perikarya and dendrites previously were found by autoradiography to contain only low densities of SRIF binding sites (e.g., pyramidal cell layer of the hippocampus) (Martin et al., 1991; Krantic et al., 1992; Moyse et al., 1992). By contrast, regions containing immunoreactive axon terminals, in which sst_{2A} receptors are likely to be mainly in membrane-associated form, were found to be intensely labeled by receptor autoradiography (Martin et al., 1991; Krantic et al., 1992; Moyse et al., 1992).

As a whole, the distribution of sst_{2A} receptor-immunoreactive perikarya correlated well with that of neurons previously found to

express sst_2 receptor mRNA by *in situ* hybridization in either mouse (Breder et al., 1992) or rat (Pérez et al., 1994; Senaris et al., 1994; Beaudet et al., 1995) brain. In fact, all areas found to contain sst_{2A} receptor-immunoreactive nerve cell bodies previously had been shown to express high levels of sst_2 receptor mRNA. However, a number of areas had been reported to express high levels of sst_2 receptor mRNA and showed either no or only low numbers of immunoreactive cells in the present study, such as layers IV and VI of the cerebral cortex, the basolateral amygdaloid nucleus, the claustrum, the endopiriform nucleus, and the hypothalamus. Interestingly, all of these areas exhibited moderate to high concentrations of sst_{2A} receptor-immunoreactive terminals, suggesting that the receptor protein might have been addressed specifically to axons of sst_{2A} receptor-expressing cells that were arborizing locally. It is also possible that regions expressing high levels of sst_2 mRNA but lacking perikaryal sst_{2A} receptor immunoreactivity selectively expressed the sst_{2B} splice variant, which does not contain the immunogenic peptide sequence. Indeed, both sst_{2A}-and sst_{2B}-expressing cells would have been recognized by the probes used in published *in situ* hybridization studies. This latter interpretation seems particularly likely in the case of the hypothalamus, in which the sst_{2B} splice variant has been suggested by Northern blotting to be expressed predominantly (Patel et al., 1993; Kong et al., 1994) and in which SRIF binding sites have been localized to nerve cell bodies by autoradiography (Epelbaum et al., 1989; McCarthy et al., 1992). This interpretation could imply that different splice variants of the sst_2 receptor are involved in the transduction of the neural and neuroendocrine functions of SRIF.

In summary, the present results demonstrate that the sst_{2A} receptor is associated with both somatodendritic and axonic elements, suggesting that it is involved in the transduction of both pre- and postsynaptic effects of SRIF in the mammalian brain. The widespread distribution of the sst_{2A} receptor in cerebral cortex and limbic structures suggests that this receptor plays a critical role in mediating SRIF effects on cognition, expression of emotional behavior, learning, and memory. These findings, together with the development of more subtype-specific SRIF analogs, should provide pharmacological strategies for the treatment of neurological and psychiatric disorders involving alterations in the somatostatinergic system, such as epilepsy, depression, and Alzheimer's disease.

REFERENCES

Adams JC (1992) Biotin amplification of biotin and horseradish peroxidase signals in histochemical stains. J Histochem Cytochem 40:1457–1463.

Arvidsson U, Riedl M, Chakrabarti S, Vulchanova L, Lee JH, Nakano AH, Lin X, Loh HH, Law PY, Wessendorf MW, Elde R (1995) The kappa-opioid receptor is primarily postsynaptic: combined immunohistochemical localization of the receptor and endogenous opioids. Proc Natl Acad Sci USA 92:5062–5066.

Beaudet A, Greenspun D, Raelson J, Tannenbaum GS (1995) Patterns of expression of SSTR1 and SSTR2 somatostatin receptor subtypes in the hypothalamus of the adult rat: relationship to neuroendocrine function. Neuroscience 65:551–561.

Breder CD, Yamada Y, Yasuda K, Seino S, Saper CB, Bell GI (1992) Differential expression of somatostatin receptor subtypes in brain. J Neurosci 12:3920–3934.

Brown PJ, Lee AB, Norman MG, Presky DH, Schonbrunn A (1990) Identification of somatostatin receptors by covalent labeling with a novel photoreactive somatostatin analog. J Biol Chem 265:17995–18004.

Bruno JF, Xu Y, Song J, Berelowitz M (1992) Molecular cloning and functional expression of a brain-specific somatostatin receptor. Proc Natl Acad Sci USA 89:11151–11155.

Epelbaum J, Moyse E, Tannenbaum GS, Kordon C, Beaudet A (1989) Combined autoradiographic and immunohistochemical evidence for an association of somatostatin binding sites with growth hormone-released factor-containing nerve cell bodies in the rat arcuate nucleus. J Neuroendocrinol 1:109–115.

Epelbaum J, Dournaud P, Fodor M, Viollet C (1994) The neurobiology of somatostatin. Crit Rev Neurobiol 8:25–44.

Göthert M (1980) Somatostatin selectively inhibits noradrenaline release from hypothalamic neurones. Nature 288:86–88.

Gu WZ, Brown PJ, Loose-Mitchell DS, Stork PJS, Schonbrunn A (1995) Development and use of a receptor antibody to characterize the interaction between somatostatin subtype 1 and G proteins. Mol Pharmacol 48:1004–1014.

Hoyer D, Lubbert H, Bruns C (1994) Molecular pharmacology of somatostatin receptors. Naunyn Schmiedebergs Arch Pharmacol 350:441–453.

Hoyer D, Bell GI, Berelowitz M, Epelbaum J, Feniuk W, Humphrey PPA, O'Carroll AM, Patel YC, Schonbrunn A, Taylor JE, Reisine T (1995) Classification and nomenclature of somatostatin receptors. Trends Pharmacol Sci 13:61–69.

Jacquin T, Champagnat J, Madamba S, Denavit-Saubier M, Siggins GR (1988) Somatostatin depresses excitability in neurons of the solitary tract complex through hyperpolarization and augmentation of I_M, a non-inactivating voltage-dependent outward current blocked by muscarinic agonists. Proc Natl Acad Sci USA 85:948–952.

Kimura N (1989) Developmental change and molecular properties of somatostatin receptors in the rat cerebral cortex. Biochem Biophys Res Commun 160:72–78.

Kluxen FW, Bruns C, Lubbert H (1992) Expression cloning of a rat brain somatostatin receptor cDNA. Proc Natl Acad Sci USA 89:4618–4622.

Koch BD, Schonbrunn A (1984) The somatostatin receptor is directly coupled to adenylate cyclase in GH4C1 pituitary cell membranes. Endocrinology 114:1784–1790.

Koch BD, Dorflinger LJ, Schonbrunn A (1985) Pertussis toxin blocks both cyclic AMP-mediated and cyclic AMP independent actions of somatostatin: evidence for coupling of Ni to decreases in intracellular free calcium. J Biol Chem 260:13138–13145.

Kong H, DePaoli AM, Breder CD, Yasuda K, Bell GI, Reisine T (1994) Differential expression of messenger RNAs for somatostatin receptor subtypes SSTR1, SSTR2, and SSTR3 in adult rat brain: analysis by RNA blotting and *in situ* hybridization histochemistry. Neuroscience 59:175–184.

Krantic S, Quirion R, Uhl G (1992) Somatostatin receptors. In: Handbook of chemical neuroanatomy, Vol II, Neuropeptide receptors in the CNS (Björklund A, Hökfelt T, Kuhar MJ, eds), pp 321–346. Amsterdam: Elsevier Science.

Laemmli UK (1970) Cleavage of structural proteins during the assembly of the head of bacteriophage T4. Nature 227:680–685.

Lamberts S, Krenning E, Reubi JC (1991) The role of somatostatin and its analogs in the diagnosis and treatment of tumors. Endocr Rev 12:450–482.

Lerner RA, Gree N, Alexander H, Liu FT, Sutcliffe JG, Shinnick TM (1981) Chemically synthesized peptides predicted from the nucleotide sequence of the hepatitis B virus genome elicit antibodies reactive with the native envelope protein of Dane particles. Proc Natl Acad Sci USA 78:3403–3407.

Levey AI, Kitt CA, Simonds WF, Price DL, Brann MR (1991) Identification and localization of muscarinic acetylcholine receptor proteins in brain with subtype-specific antibodies. J Neurosci 11:3218–3226.

Levey AI, Hersch SM, Rye DB, Sunahara RG, Niznik HB, Kitt CA, Price DL, Maggio R, Brann MR, Ciliax BJ (1993) Localization of D_1 and D_2 dopamine receptors in brain with subtype-specific antibodies. Proc Natl Acad Sci USA 90:8861–8865.

Martin JL, Chesselet MF, Raynor K, Gonzales C, Reisine (1991) Differential distribution of somatostatin receptor subtypes in rat brain revealed by newly developed somatostatin analogs. Neuroscience 41:581–593.

McCarthy GF, Beaudet A, Tannenbaum GS (1992) Co-localization of somatostatin receptors and growth hormone-releasing factor immunoreactivity in neurons of the rat arcuate nucleus. Neuroendocrinology 56:18–24.

Moyse E, Beaudet A, Bertherat J, Epelbaum J (1992) Light microscopic radioautographic localization of somatostatin binding sites in the brainstem of the rat. J Chem Neuroanat 5:75–84.

Novikoff AB, Novikoff PM, Quintana N, Davis C (1972) Diffusion artifacts in 3,3′-diaminobenzidine cytochemistry. J Histochem Cytochem 20:745–749.

O'Carroll A-M, Lolait SJ, Konig M, Mahan LC (1992) Molecular cloning and expression of a pituitary somatostatin receptor with preferential affinity for somatostatin-28. Mol Pharmacol 42:939–946.

Olpe HR, Steinmann MW, Pozza MF, Haas HL (1987) Comparative investigations on the actions of ACTH1–24, somatostatin, neurotensin, substance P, and vasopressin on locus coeruleus neuronal activity *in vitro*. Naunyn Schmiedebergs Arch Pharmacol 336:434–437.

Patel YC, Greenwood M, Kent G, Panetta R, Srikant CB (1993) Multiple gene transcripts of the somatostatin receptor SSTR2: tissue selective distribution and cAMP regulation. Biochem Biophys Res Commun 192:288–294.

Patel YC, Panetta R, Escher E, Greenwood M, Srikant CB (1994) Expression of multiple somatostatin receptor genes in AtT-20 cells. Evidence for a novel somatostatin-28 selective receptor subtype. J Biol Chem 269:1506–1509.

Pérez J, Rigo M, Kaupmann K, Bruns C, Yasuda K, Bell GI, Lubbert H, Hoyer D (1994) Localization of somatostatin (SRIF) SSTR-1, SSTR-2, and SSTR-3 receptor mRNA in rat brain by *in situ* hybridization. Naunyn Schmiedebergs Arch Pharmacol 349:145–160.

Perlman JH, Nussenzveig DR, Osman R, Gershengorn MC (1992) Thyrotropin releasing hormone binding to the mouse pituitary receptor does not involve ionic interactions. A model for neutral peptide binding to G protein-coupled receptors. J Biol Chem 267:24413–24417.

Pollard JW, Luqmani Y, Bateson A, Chotai K (1984) DNA transformation of mammalian cells. In: Methods in molecular biology, Vol 2 (Walker JM, ed), pp 321–332. Clifton, NJ: Humana.

Reisine T, Bell GI (1995) Molecular properties of somatostatin receptors. Neuroscience 67:777–790.

Reisine T, Kong H, Raynor K, Yano H, Takeda J, Yasuda K, Bell GI (1993) Splice variant of the somatostatin receptor 2 subtype, somatostatin receptor 2B, couples to adenylyl cyclase. Mol Pharmacol 44:1016–1020.

Sakamoto C, Nagao M, Matozaki T, Nishizaki H, Kondo Y, Baba S (1988) Somatostatin receptors on rat cerebrocortical membranes: structural characterization of somatostatin-14 and somatostatin-28 receptors and comparison with pancreatic type receptors. J Biol Chem 263:14441–14445.

Schonbrunn A, Gu YZ, Brown PJ, Loose-Mitchell D (1995) Function and regulation of somatostatin receptor subtypes. In: Somatostatin and its receptors, Vol 190 (Chadwick DJ, Cardew G, eds), pp 204–221. Chichester, UK: Wiley.

Schweitzer P, Madamba S, Siggins GR (1990) Arachidonic acid metabolites as mediators of somatostatin-induced increase of neuronal M-current. Nature 346:464–467.

Schweitzer P, Madamba S, Champagnat J, Siggins GR (1993) Somatostatin inhibition of hippocampal CA1 pyramidal neurons: mediation by arachidonic acid and its metabolites. J Neurosci 13:2033–2049.

Senaris RM, Humphrey PPA, Emson PC (1994) Distribution of somatostatin receptors 1, 2, and 3 mRNA in rat brain and pituitary. Eur J Neurosci 6:1883–1896.

Sesack SR, Aoki C, Pickel VM (1994) Dopamine receptor-like immunolabeling in midbrain and striatum. J Neurosci 14:88–106.

Tanaka S, Tsujimoto A (1981) Somatostatin facilitates the serotonin release from rat cerebral cortex, hippocampus, and hypothalamus slices. Brain Res 208:219–222.

Theveniau M, Yasuda K, Bell GI, Reisine T (1994) Immunological detection of isoforms of the somatostatin receptor subtype, SSTR2. J Neurochem 63:447–455.

Tomura H, Okajima F, Akbar M, Majid MA, Sho K, Kondo Y (1994) Transfected human somatostatin receptor type 2, SSTR2, not only inhibits adenylate cyclase but also stimulates phospholipase C and Ca^{2+} mobilization. Biochem Biophys Res Commun 200:986–992.

Twery MJ, Wong LA, Gallagher JP (1991) Somatostatin-induced hyperpolarization of septal neurons is not blocked by pertussis toxin. Eur J Pharmacol 192:287–291.

Vanetti M, Kouba M, Wang X, Vogt G, Höllt V (1992) Cloning and expression of a novel mouse somatostatin receptor (SSTR2B). FEBS Lett 311:290–294.

Vanetti M, Vogt G, Höllt V (1993) The two isoforms of the mouse somatostatin receptor (mSSTR2A and mSSTR2B) differ in coupling efficiency to adenylate cyclase and in agonist-induced receptor desensitization. FEBS Lett 331:260–266.

Vanetti M, Ziolkowska B, Wang X, Horn G, Höllt V (1994) mRNA distribution of two isoforms of somatostatin receptor 2 (mSSTR2A and mSSTR2B) in mouse brain. Mol Brain Res 27:44–50.

Yamada Y, Post SR, Wang K, Tager HS, Bell GI, Seino S (1992) Cloning and functional characterization of a family of human and mouse somatostatin receptors expressed in brain, gastrointestinal tract, and kidney. Proc Natl Acad Sci USA 89:251–255.

Yasuda K, Rens-Domiano S, Breder CD, Law SF, Saper CB, Reisine T, Bell GI (1992) Cloning of a novel somatostatin receptor, SSTR3, coupled to adenylylcyclase. J Biol Chem 267:20422–20428.

Xie Z, Sastry BR (1992) Actions of somatostatin on GABA-ergic synaptic transmission in the CA1 area of the hippocampus. Brain Res 591: 239–247.